Coupling of Cyclic Voltammetry and Electrochemical Impedance Spectroscopy for Probing the Thermodynamics of Facilitated Ion Transfer Reactions Exhibiting Chemical Kinetic Hindrances

Rubin Gulaboski,*,†,‡,|| Elisabete S. Ferreira,† Carlos. M. Pereira,*,† M. Natalia D. S. Cordeiro,‡ Alessandra Garau,§ Vito Lippolis,§ and A. F. Silva†

CIQ-UP L4, Faculdade de Ciências, Universidade do Porto, Rua do Campo Alegre, 687, 4169-007 Porto, Portugal, REQUIMTE, Faculdade de Ciências, Universidade do Porto, Rua do Campo Alegre, 687, 4169-007 Porto, Portugal, Dipartimento di Chimica Inorganica ed Analitica, Università degli Studi di Cagliari, S.S. 554 Bivio per Sestu, 09042 Monserrato (CA), Italy

Received: August 2, 2007; In Final Form: September 20, 2007

Mathematical models under conditions of cyclic staircase voltammetry and electrochemical impedance spectroscopy (EIS), which consider the kinetic effects due to the complexation reaction by the facilitated transfer of metal ions at polarized interfaces, are presented. Criteria for qualitative recognition of these kinetic effects from the features of simulated cyclic voltammograms are given. In case of the existence of these effects, only the EIS can bring access to the thermodynamics and kinetics of the complexation chemical reaction. Analytical equations for estimating the thermodynamic parameters by such systems under EIS conditions are evaluated. The theoretical results are compared with the experimental results of the facilitated Cu^{2+} transfer at the polarized water−1,2-dichlorethane interface, assisted by two phenanthroline-containing macrocycles. In the experimental case where kinetic effects due to the complexation step exist, we show how elegantly EIS can be used as a tool for estimation of the complexation constant of Cu^{2+} and 5-oxo-2,8-dithia [9],(2,9)-1,10-phenanthrolinophane ($PhenOS_2$).

1. Introduction

The processes of ion transfer across a liquid−liquid interface attract considerable interest due to their potential application in a diverse number of fields such as metal extraction,[1] ion-sensitive electrodes,[2] drug delivery and drug design,[3] and many others.[4−6] Electrochemical studies on the facilitated transfer of various ions across liquid−liquid interfaces have been extensively reported in the literature.[1,2,6] Ion transfer followed by complexation or by ion-pair formation is one of the most widely encountered examples of reactions taking place at polarized liquid−liquid interfaces.[5,6] The assisted ion transfer with the help of various neutral ionophores such as crown ethers,[6−9] calixarenes,[10] azines,[11−14] or phenantrolines[15−17] has been studied mainly by cyclic voltammetry at a polarized liquid−liquid interface. The efficiency of a given ligand L to act as a facilitating agent in ion-extraction processes is portrayed through the value of the thermodynamic complexation constant.[2,5,18,19] The higher the value of the complexation (formation) constant, the higher the efficiency of the ion extraction with a given ligand. For the determination of the complexation constants by facilitated ion-transfer (FIT) voltammetric experiments at polarized liquid−liquid interfaces, the modified versions of the DeFord−Hume polarographic method are extensively used.[2,5,6,18] The facilitated ion transfer processes are often considered as multistep systems comprising: (i) ion transfer across the liquid−liquid interface and (ii) chemical reaction (complexation) of the transferred ion with the ionophore (ligand). If this holds true, then the facilitated ion transfer processes can be thought to take place according to an EC mechanism, where the ion transfer is the electrochemical (E) step, and the consecutive complexation of the ion by the ionophore is a chemical step (C).[5,6,20,21] It is worth mentioning that, beside this EC consideration, cases exist where the CE mechanism is also proposed as an adequate model for describing the facilitated ion transfer reactions.[21] In that case, usually the ligand (ionophore) is partitioned from the organic in the water phase, while forming there a charged complex with the metal ions (C step). The transfer of that charged complex across the liquid−liquid interface is considered as electrochemical (E-step). These situations are nicely described in the work of Girault et al.[21] Whether one facilitated ion transfer process can be regarded as an EC or CE reaction, the best arguments can be found in the features of the cyclic voltammograms, indeed, since those are quite different for the two systems.[22] It is worth mentioning that the first theory for cyclic linear sweep voltammetry of facilitated ion transfer reactions across the water−organic liquid interface, with different ion:ionophore stoichiometries, has been established by Homolka et al.[23] The main conclusion of the work[23] was to relate the peak-to-peak separation to the complexation stoichiometry. However, neither in ref 23 nor in ref 21 have the authors considered the chemical kinetic effects to the theoretical voltammetric features of these systems. In most of the references reporting on FIT, the mathematical approaches for the characterization of the formed complexes in cyclic voltammetry experiments are based on pure thermodynamic (Nernstian) principles, neglecting often kinetic effects.[2,5,6,18,21,23] If, however, the FIT is regarded as an EC two-

* Corresponding authors. E-mail: cmpereir@fc.up.pt; rgulaboski@fc.up.pt.
† CIQ-UP L4, Faculdade de Ciências, Universidade do Porto.
‡ REQUIMTE, Faculdade de Ciências, Universidade do Porto.
§ Università degli Studi di Cagliari.
|| On leave from the FON-First Private University, Skopje, Macedonia, and Department of Chemistry, Faculty of Natural Sciences and Mathematics, University Sts "Kiril i Metodij", Skopje, Macedonia.

10.1021/jp076203s CCC: $40.75
Published on Web 12/13/2007

step process,[20,21] then at least two kinetic effects should be considered: (i) kinetic constraints due to the slow ion transfer reaction and (ii) kinetic "hindrances" produced by the chemical (complexation) step.[20,22] Although the kinetic effects due to the slow ion transfer have been studied with several electroanalytical techniques[5,20,24−26] and scanning electron microscopy,[27] up to now, there is no reference in the literature considering the kinetic effects due to the "hindrances" at the complexation step in FIT experiments. This fact is rather surprising, knowing that kinetic effects due to the occurrence of a complexation reaction between two species (usually a metal M and a ligand L) are very often encountered in these kinds of experiments.[15,19,20,28−33] When dealing with FIT experiments, it is very difficult to distinguish the kinetic effects due to the chemical complexation from those related to the ion transfer step, and only people skilled in voltammetric techniques can recognized them. However, neglecting these effects in the mathematical models of FIT can lead to misinterpretations and incorrect values of the estimated thermodynamic parameters in the experiments. With this in mind, we are presenting key results from mathematical models developed under conditions of cyclic voltammetry and electrochemical impedance spectroscopy, which are considering the kinetic effects due to chemical complexation at facilitated ion transfer processes. We give a set of simple voltammetric diagnostic criteria for qualitative recognition of the involved kinetic in the chemical step of FIT experiments, while presenting an elegant manner to access the thermodynamics and kinetics of the complexation reaction from the EIS experiments. We also present experimental evidence of these phenomena, in the case of facilitated ion transfer of Cu^{2+} with two different phenanthroline-containing macrocyclic ligands, taking place at the polarized water-1,2-dichlorethane interface.

2. Mathematical Models

2.1. Cyclic Voltammetry. *2.1.1. Cyclic Voltammetry of Facilitated Ion Transfer at Polarized Liquid−Liquid Interface: Ion Transfer Coupled to a Subsequent Complexation Reaction.* We consider here a situation of a reversible (kinetically unhindered) ion transfer of a metal ion M, which is facilitated by a highly lipophilic ligand L, present in the organic phase only. This situation can be presented by the following reaction scheme:

$$M_{(w)} \leftrightarrow M_{(o)} + L_{(o)} \underset{k_b}{\overset{k_f}{\rightleftarrows}} ML_{(o)} \qquad (I)$$

where M is some metal ion initially present in the water phase (w) and L is a ligand present in the organic phase (o), and ML is the formed complex between them (charges and stoichiometric coefficients are omitted for simplicity). It is worth noting that this model corresponds to cases where the complexation process between M and L takes place in the organic phase only, which is mostly encountered experimental situation.[2,5,6,18,21] k_f (s^{-1}) and k_b (s^{-1}) are the first-order chemical rate constants (forward and backward, respectively) of the complexation reaction between M and L in the organic phase. In practice, the forward chemical reaction is of higher-order, and it is defined as $k_f = k_f'c(L)c(M)$. Usually, in case of excess concentration of one of the participants (M or L), the expression for the chemical rate constant is simplified to $k_f = k_f'c(L)$ (or $k_f = k_f'c(M)$). In this case, k_f' is the real chemical rate constant, with units of $mol^{-1}cm^3\ s^{-1}$ (if the concentration is expressed in mol cm^{-3}). We assume that the mass transfer occurs exclusively by diffusion. Therefore, the application of the second Fick's law to any species involved in the reaction Scheme 1 leads to the following differential equations:

SCHEME 1: Chemical Structures of $PhenS_2$ and $PhenOS_2$ Ligands

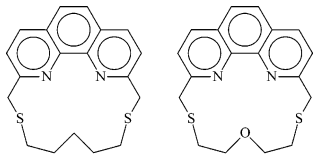

$$\frac{\partial c_{M_{(w)}}}{\partial t} = D_{M(w)}\frac{\partial^2 c_{M_{(w)}}}{\partial x^2} \qquad (1)$$

$$\frac{\partial c_{M_{(o)}}}{\partial t} = D_{M_{(o)}}\frac{\partial^2 c_{M_{(o)}}}{\partial x^2} - k_f c_{M_{(o)}} + \frac{k_f}{K} c_{ML_{(o)}} \qquad (2)$$

$$\frac{\partial c_{ML_{(o)}}}{\partial t} = D_{ML_{(o)}}\frac{\partial^2 c_{ML_{(o)}}}{\partial x^2} + k_f c_{M_{(o)}} - \frac{k_f}{K} c_{ML_{(o)}} \qquad (3)$$

where $K = k_f/k_b$ (or $K = c(M)_o/c(ML)_o$ for the particular case in Scheme 1) is the equilibrium constant of the complexation reaction (i.e., the instability constant), which follows the ion transfer step in the reaction scheme (I), and D is the diffusion coefficient (it is assumed to have equal value in both water and organic phase). The differential equations (1−3) have been solved under the following boundary conditions:

$$t = 0,\ x \geq 0,\ c(M_{(w)}) = c(M_{(w)})^*,\quad c(M_{(o)}) = c(ML_{(o)}) = 0 \quad (a)$$

$$t > 0,\ x \to \infty,\ c(M_{(w)}) \to c(M_{(w)})^*,\quad c(M_{(o)}) = c(ML_{(o)}) \to 0 \quad (b)$$

$$t > 0,\ x = 0,\ D_{M_{(w)}}\frac{\partial c_{M_{(w)}}}{\partial x} = -D_{M_{(o)}}\frac{\partial c_{M_{(o)}}}{\partial x} = -\frac{I}{FA} \quad (c)$$

$$t > 0,\ x = 0,\ D_{ML_{(o)}}\frac{\partial c_{ML_{(o)}}}{\partial x} = D_{L_{(o)}}\frac{\partial c_{L_{(o)}}}{\partial x} = 0$$

$$\Delta_w^o\varphi = \Delta_w^o\varphi_M^\theta + \frac{RT}{F}\ln\frac{c_{M_{(w)}}}{c_{M_{(o)}}} \qquad (d)$$

where $\Delta_w^o\varphi$ is the applied potential difference at the liquid−liquid interface, $\Delta_w^o\varphi_M^\theta$ is the standard potential of ion transfer (nonfacilitated) of metal ion M from water to organic phase, $c_{M_{(o)}}$ and $c_{M_{(w)}}$ are the concentrations of the metal ion M in organic and water phase, respectively, and $c(M_{(w)})^*$ is the total (initial) concentration of the metal ion in water phase. I is the current, and A (cm^2) is the surface area of the liquid−liquid interface. R, T, and F are the gas constant, thermodynamic temperature, and Faraday constant, respectively. It is worth mentioning that the situation $x = 0$ corresponds to the liquid−liqid interface. The solutions of the differential equations (1−3), under the relevant boundary conditions, have been obtained by using the Laplace's transformations, combined with the numerical integration methodology.[20] The solutions for the concentrations of $c(M_{(w)})_{x=0}$ and $c(M_{(o)})_{x=0}$ are identical with those obtained for an EC_{rev} diffusion reaction of the type

$$\mathrm{Ox} + n\mathrm{e}^- \leftrightarrow \mathrm{Red} \underset{k_b}{\overset{k_f}{\leftrightarrows}} \mathrm{Y} \qquad \text{(II)}$$

given elsewhere[22,34,35] and they read

$$c(\mathrm{M})_{(\mathrm{w})x=0} = c(\mathrm{M})^*_{(\mathrm{w})} + \int_0^t \frac{I(t)}{nFA\sqrt{D}} \frac{1}{\sqrt{\pi(t-\tau)}}\,\mathrm{d}\tau \quad (4)$$

$$c(\mathrm{M})_{(\mathrm{o})x=0} = -\frac{1}{1+K}\int_0^t \frac{I(t)}{nFA\sqrt{D}} \frac{1}{\sqrt{\pi(t-\tau)}}\,\mathrm{d}\tau - \frac{K}{1+K}\int_0^t \frac{I(t)}{nFA\sqrt{D}} \frac{\exp(-k(t-\tau))}{\sqrt{\pi(t-\tau)}}\,\mathrm{d}\tau \quad (5)$$

where $k = k_f + k_b$ and $K = k_f/k_b$.

The solutions (4) and (5) of the metal concentrations in water (w) and organic phase (o) have been incorporated in the Nernst equation (d). The numerical solution of that equation has been obtained by the method of Nicholson and Olmstead.[36] Both variables, the dimensionless current Ψ and time t, were incremented. To each time $t = md$, where d is the time increment, a certain current Ψ_m was ascribed. The numerical solution is represented by the following recursive formula, which can be applied correspondingly to the cathodic and anodic currents of the cyclic staircase voltammograms (eq 6) where numerical integration parameters are $S_m = \sqrt{m} - \sqrt{(m-1)}$ and $M_m = erf(\sqrt{[\epsilon m/50]}) - erf(\sqrt{[\epsilon(m-1)/50]})$, and ϵ is the dimensionless chemical kinetic parameter defined as $\epsilon = k/t$. φ is the dimensionless potential, defined as $\varphi = nF/RT(\Delta^o_w\varphi - \Delta^o_w\varphi^\theta_M)$.

The dimensionless current Ψ is defined as $\Psi = (I\sqrt{t})/(FAc(\mathrm{M})^*_{(\mathrm{w})}\sqrt{D})$. It is worth noting that the above recursive formula (6) and the expressions below the formula (6) can be directly incorporated in the MATHCAD voltammetric file, as that given elsewhere.[37] The last cited paper[37] is available on-line free, and everyone having small experience with MATHCAD can do the corresponding simulations presented in this work.

The theoretical simulations have been made under conditions of cyclic staircase voltammetry. The excitation signal used in cyclic staircase voltammetry consists of a staircase potential ramp, which is characterized by the duration of the potential tread τ and the step of the staircase ramp dE. For numerical simulation, the time increments $d = \tau/25$ was used. All the simulations have been performed at temperature of $T = 298$ K.

The theoretical cyclic voltammograms are a function of the scan rate υ, as well as of the thermodynamic parameter K and kinetic parameter ϵ.[20,22,34,35] Both K and ϵ are functions of the ligand concentration in the organic phase $c(\mathrm{L})_o$. In fact, the concentration of the ligand in the organic phase $c(\mathrm{L})_o$ affects the forward rate constant of the chemical reaction (k_f'), and since K and ϵ are both defined via k_f' (see the definitions in the conditions above), it would mean that both of these parameters will be a function of $c(\mathrm{L})_o$. For this type of complexation, the real thermodynamic constant K' (i.e., the stability constant of the created ML complex) can be also defined as $K' = c(\mathrm{ML})_o/c(\mathrm{M})_o c(\mathrm{L})_o$, where $c(\mathrm{ML})_o$, $c(\mathrm{M})_o$, and $c(\mathrm{L})_o$ are the equilibrium concentrations of the complex, metal, and the ligand in the organic phase, respectively.[21] If we link the definitions given below eq 3, where we defined the dimensionless parameter K as $K = c(\mathrm{M})_o/c(\mathrm{ML})_o$ for the particular case considered, it follows that the real stability complexation constant K' is linked to the dimensionless thermodynamic parameter K with $K' = c(\mathrm{ML})_o/c(\mathrm{M})_w c(\mathrm{L})_o$, or $K' = 1/Kc(\mathrm{L})_o$. From the last equation, it follows that the dimensionless parameter K is linked to the ligand concentration and the real complexation constant as $K = 1/K'c(\mathrm{L})_o$. This last equation shows that in the simulations we can change independently the ligand concentration $c(\mathrm{L})_o$, for a given value of the real stability constant K', and following in that way the influence of K toward the voltammetric features, as this dimensionless parameter K appears in the recursive calculation of eq 6. All of the simulations have been made with the aid of the software package MATHCAD.[37] It is worth mentioning that comprehensive studies of an $E_{rev}C_{rev}$ mechanism for case of planar metallic electrodes under voltammetric conditions, which consider similar model to that presented here, can be found elsewhere.[22,34,35] That is the reason why we emphasize in this work only the key phenomena that are of benefit for the particular case of chemical kinetics by the assisted ion transfer processes.

2.1.2. Theoretical Cyclic Voltammograms in the Absence of Kinetic Effects. We give here some representative cyclic voltammograms and a brief discussion for common thermodynamic situations regarding the case of the absence of kinetic effects in the considered facilitated metal−ion transfer across the polarized liquid−liquid interface. The region of absence of kinetic effects is chosen from the diagrams showing the dependence of peak-currents and peak potentials vs the kinetic parameter, as those given elsewhere.[34,35] The discussion in this part of the paper emphasizes the influence of the ligand concentration in the organic phase to the features of the cyclic voltammograms. Bearing in mind the definitions for K and k_f (see above), both K and ϵ are a function of the concentration of the ligand $c_{(\mathrm{L})}$. Therefore, for this particular system, it is worth investigating the influence of the ligand concentration $c_{(\mathrm{L})}$ on the theoretical voltammetric responses, as this is common in FIT experiments.[2,5,6,8,17,18,21,23] If there is an absence of kinetic effects by the complexation reaction, then conventional cyclic voltammograms possessing electrochemically reversible features are obtained,[21,23,34] as those given in Figure 1A. Although the peak currents do not vary by changing the ligand concentration, the mid-peak potentials of the theoretical voltammograms shift in the negative direction by increasing the concentration of the ligand L in the organic phase.[21] This is a well-known thermodynamic shift, from which one can estimate the stoichiometry of the complex formed, as well as the thermodynamic complexation constant.[2,8,18,21,23] Various considered cases for the estimation of these parameters can be found in the excellent papers of Girault et al.[8,17,18,21] The mid-peak potentials of the simulated cyclic voltammograms are a linear function of the logarithm of the ligand concentration (Figure 1B), with slope defined as mRT/zF, where z is the charge number of the metal ion transferred and m is the number of ligand molecules bind

$$\Psi_m = \frac{-\frac{2}{\sqrt{50\pi}}\left(\frac{1}{1+K} + \exp(\varphi_m)\right)\sum_{j=1}^{m-1}\Psi_j S_{m-j+1} - \frac{K}{(1+K)\sqrt{\epsilon}}\sum_{j=1}^{m-1}\Psi_j M_{m-j+1} + \exp(\varphi_m)}{\frac{2}{\sqrt{50\pi}}\left(\frac{1}{1+K} + \exp(\varphi_m)\right) + \frac{KM_1}{(1+K)\sqrt{\epsilon}}} \quad (6)$$

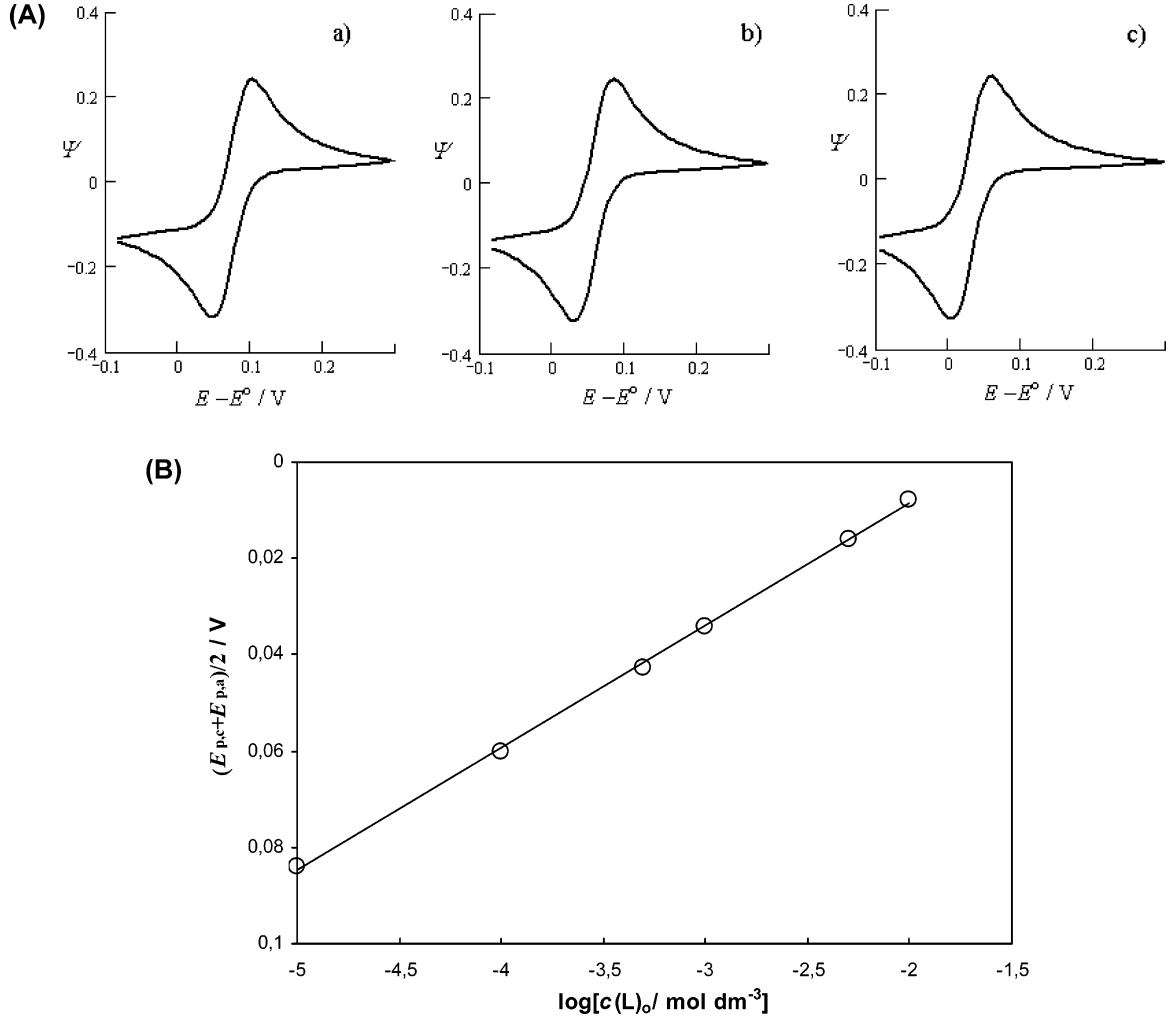

Figure 1. (A) Simulated cyclic voltammograms for facilitated ion transfer reaction of M^{2+} ion obtained by increasing the ligand concentration in the organic phase, in absence of any kinetic effects. Scan rate $\upsilon = 20$ mV/s, potential increment d$E = 4$ mV, $T = 298$ K, the value of the real complexation constant in the simulations was $K' = 10^8$ mol^{-1} dm,^{3} $D = 5 \times 10^{-6}$ cm^2 s^{-1}. The concentration of the ligand is c(L)/mol dm^{-3} = 0.00001 (a), 0.0001 (b), and 0.001 (c). (Ψ is the dimensionless current at the cyclic voltammograms). (B) Dependence of the mid-peak potential ($E_{p,c} + E_{p,a}$)/2 of the cyclic voltammograms on the ligand concentration in the organic phase.

to the metal ion M. R, T, and F are the gas constant, thermodynamic temperature, and Faraday constant, respectively. The intercept of this linear dependence is defined as $(-RT/zF)$ ln(K_m), from which the value of the complexation constant K_m can be deduced.[17,18,21] Therefore, for the system considered, the variation of the mid-peak potential plotted as a function of log-($c_{(L)}$) gives the number of the ligand molecules in the complex, m, (deduced from the slope) as well as the value of the thermodynamic complexation constant, K_m (calculated from the intercept).

It is worth mentioning at this point that the mid-peak potential of the cyclic voltammograms will shift with the value of the dimensionless parameter K following the equation:

$$\Delta^{o}_{w}\varphi_{1/2} = \Delta^{o}_{w}\varphi(M)^{\theta} + \frac{RT}{F}\ln\left(\frac{K}{1+K}\right) \qquad (7)$$

Let us remind that, in the definitions in this mathematical model, we defined the dimensionless parameter K as $K = 1/K'c(L)_o$. This equation shows that, by increasing the concentration of the ligand $c(L)_o$, the dimensionless parameter K will decrease and will be smaller than 1 for stable complexes and concentrations usually used in these types of electrochemical experiments. Therefore, as the $c(L)_o$ increases, the term $K/(1 + K)$ in eq 7 will decrease, and it will get positive values smaller than 1. Consequently, the logarithmic term ln[$K/(1 + K)$] in eq 7 will become more negative by increasing the ligand concentration. The final output of this effect in eq 7 will be portrayed in a shift of the mid-peak potentials of cyclic voltammograms toward more negative values (versus the standard redox potential of the system), as it has been observed by the simulated voltammograms presented in Figure 1A.

2.1.3. Theoretical Cyclic Voltammograms in the Presence of Kinetic Effects Due To a Complexation Reaction Subsequent to the Ion-Transfer Step. Several cyclic voltammograms simulated for different ligand concentrations, in the presence of kinetic hindrances due to the occurrence of the follow-up chemical reaction in reaction Scheme 1, are shown in Figure 2. In such a case, at least two distinctive features in the cyclic voltammograms can be observed: (a) the peak currents are sensitive to the concentration of the ligand, and they decrease by increasing the ligand concentration and (b) the mid-peak potentials of the cyclic voltammograms are almost insensitive to the changes in ligand concentration, producing a slight shift toward positive values by increasing the ligand concentration. Moreover, there are also obvious changes in the shape of the anodic peaks that assume more flattened form at higher ligand concentrations due to the presence of kinetic hindrances.[22,34] The features of the cyclic voltammograms in this case are just

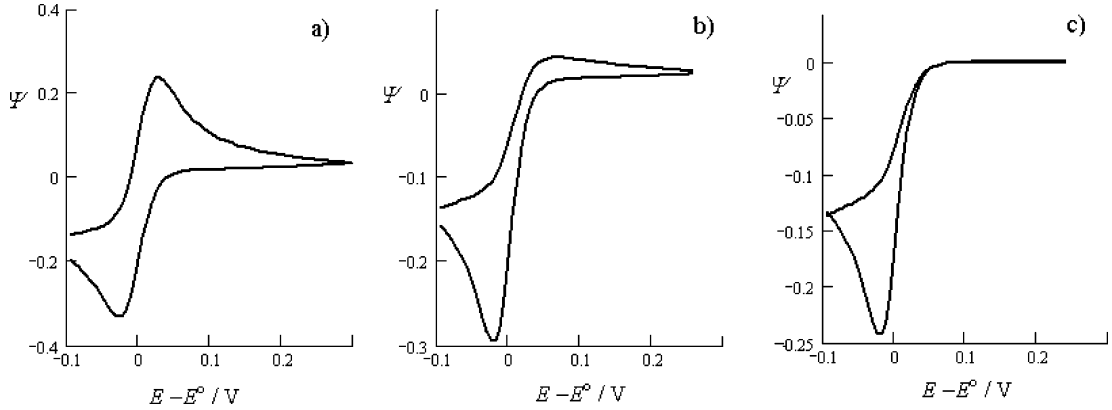

Figure 2. Simulated cyclic voltammograms for facilitated ion transfer reaction of the M^{2+} ion obtained by increasing the ligand concentration in the organic phase, in the presence of kinetic effects due to the chemical complexation reaction. Scan rate $v = 20$ mV/s, potential increment $dE = 4$ mV, $T = 298$ K, the value of the real complexation constant in the simulations was $K' = 10^8$ mol^{-1} dm,^{3} $k_f' = 10^{1.2}$ mol^{-1}cm^3 s^{-1}, $D = 5 \times 10^{-6}$ cm^2 s^{-1}. The concentration of the ligand is c(L)/mol dm^{-3} = 0.00001 (a), 0.0001 (b), and 0.001 (c).

opposite to those observed in the absence of kinetic restraints (compare with voltammograms in Figure 1A). In practice, this would explicitly mean that changing the ligand concentration in the organic phase would not cause a shift of the half-peak potentials in cyclic voltammograms (or would cause a slight shift of the mid-peak potential in the positive, and not the negative direction). It is worth reminding that the potential shift by changing the ligand concentration is a crucial feature for the estimation of the complexation constant. The main reason for this anomalous behavior of such systems is the simultaneous effect on the kinetics (via chemical kinetic parameter ϵ) and thermodynamics (via K) by the ligand concentration.[20,22,34,35] Both phenomena shift the mid-peak potential by about the same values but in opposite directions. The outcome of this is the absence of the mid-peak potential shifting at the cyclic voltammograms.[34,35] In such cases, cyclic voltammetry will be useless for the estimation of the thermodynamics parameters for the ion complexation, and a more rigorous treatment of the data is needed in order to obtain the value of K. We present below a model developed under electrochemical impedance spectroscopy, which can be elegantly used for resolving of the thermodynamics of facilitated ion transfer considered above.

2.2. Electrochemical Impedance Spectroscopy. In the last several decades, the electrochemical impedance spectroscopy (EIS) has been promoted as a powerful tool for probing into various electrochemical systems.[38] Many advantages accrue from this technique. Among the most important are (a) the experimental ability to make high-precision measurements, because the response may be indefinitely steady and can therefore be averaged over a long term, (b) an ability to treat the response theoretically by linearized current−potential characteristics, and (c) measurements over a high-frequency range. Since one usually works close to equilibrium, no detailed knowledge about the behavior of the $I-E$ response curve at higher and lover overpotentials is required. This advantage leads to important simplifications in treating the kinetic features by various systems.[20,38−40] In general, an equivalent circuit composed of resistors and capacitors represents the features of an electrochemical system in EIS.[38−40] A main problem often encountered in the frequency domain EIS is the difficulty of determining the "uniqueness" of the circuit-model obtained from experimental data. Although large numbers of equivalent circuits have been devised to account for rather complex electrochemical systems,[38−42] only in the simplest cases can one identify individual circuit elements with processes that occur in the electrochemical cell. This is especially true for equivalent

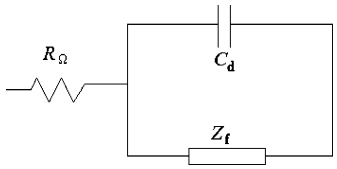

Figure 3. Scheme of the Randles equivalent circuit used in EIS.

circuits representing more complicated processes, such those of the coupled homogeneous reactions, for example.[38−42] In this work, we have chosen the most common Randles equivalent circuit as a corresponding one for the system considered. We show that the main kinetic and thermodynamic features of the facilitated ion transfer reaction described by reaction Scheme 1 can be elegantly evaluated from the frequency dependences of the real and imaginary part of the impedance.

2.2.1. Electrochemical Impedance Spectroscopy of Facilitated Ion Transfer at the Polarized Liquid−Liquid Interface-Ion Transfer Coupled by Follow-Up Chemical Reaction. We consider again an electrochemical system of a thermodynamically reversible ion transfer of a metal ion M, which is facilitated with a highly lipophilic ligand L (M:L stochiometry of the complex is 1:1), as in the voltammetric model described above

$$M_{(w)} \leftrightarrow M_{(o)} + L_{(o)} \underset{k_b}{\overset{k_f}{\rightleftarrows}} ML_{(o)} \qquad (I)$$

In EIS, this situation can be represented by simple Randles equivalent circuit[20,22,38] (see Figure 3). For solving this problem under conditions of EIS, one needs solutions for the time-dependent concentrations of the metal M in water and the organic phase, respectively. For the considered system described by reaction scheme I, these solutions are equivalent to those for a reversible electrochemical reaction that is coupled with subsequent chemical reaction,[42] and they read

$$c(M)_{(w)} = c^* - \frac{I}{zFA\sqrt{2D\omega}}[\sin(\omega t) - \cos(\omega t)] \qquad (8)$$

where ω is the frequency, A is the surface area of the liquid−

$$c(M)_{(o)} = \frac{I}{zFA\sqrt{2D\omega}}\frac{K}{(1+K)}[\sin(\omega t) - \cos(\omega t)] + \frac{1}{(1+K)}\frac{1}{\sqrt{\epsilon}}\frac{I}{zFS\sqrt{2D}}[\sin(\omega t) - \cos(\omega t)] \qquad (9)$$

liquid interface, K is the thermodynamic constant defined as K

$= k_f/k_b$, and ϵ is chemical kinetic parameter defined as $\epsilon = k_f + k_b$. The other symbols have their usual meaning. The time-differentiation of eqs 8 and 9 leads to

$$\frac{dc(M)_{(w)}}{dt} = \frac{I}{nFA}\sqrt{\frac{\omega}{2D}}[\sin(\omega t) + \cos(\omega t)] \quad (10)$$

$$\frac{dc(M)_{(o)}}{dt} = \frac{I\sqrt{\omega}}{zFA\sqrt{2D}}\frac{K}{(1+K)}[\sin(\omega t) + \cos(\omega t)] + \frac{1}{(1+K)}\frac{1}{\sqrt{\epsilon}}\frac{I\omega}{zFA\sqrt{2D}}[\sin(\omega t) + \cos(\omega t)] \quad (11)$$

For the Randles circuit, the expression for the time-dependent potential is given by[38]

$$\frac{dE}{dt} = R_{ct}\frac{dI}{dt} + \beta_1\frac{dc(M)_{(w)}}{dt} + \beta_2\frac{dc(M)_{(o)}}{dt} \quad (12)$$

R_{ct} is the charge-transfer resistance, and the constants β_1 and β_2 are defined as $\beta_1 = RT/Fc'(M)_{(w)}$ and $\beta_2 = RT/Fc'(M)_{(o)}$ ($c'(M)_{(w)}$ and $c'(M)_{(o)}$ are equilibrium concentrations of M in water and organic phase, respectively). D is the common diffusion coefficient of metal ion M, which is assumed to be equal in both water and organic phase.

Since a sinusoidal type of current with form of $I = I_o \sin(\omega t)$ is forced through the circuit (I_o is the current amplitude), the expression for dI/dt in eq 12 is

$$\frac{dI}{dt} = I_o\omega\cos(\omega t) \quad (13)$$

by substituting of eqs 10, 11, and 13, into the eq 12, and after rearrangements, one gets

$$\frac{dE}{dt} = I_o\omega\cos(\omega t)\left[R_{ct} + \frac{\beta_1}{zFA\sqrt{2D\omega}} + \frac{\beta_2}{zFA\sqrt{2D\omega}}\frac{K}{(1+K)} + \frac{\beta_2}{zFA\sqrt{2D}}\frac{1}{(1+K)\sqrt{\epsilon}}\right] + I_o\sqrt{\omega}\sin(\omega t)\left[\frac{\beta_1}{zFA\sqrt{2D\omega}} + \frac{\beta_2}{zFA\sqrt{2D\omega}}\frac{K}{(1+K)} + \frac{\beta_2}{zFA\sqrt{2D}}\frac{\sqrt{\omega}}{(1+K)\sqrt{\epsilon}}\right] \quad (14)$$

From the other side, the total voltage drop across the faradaic element of the Randles circuit given in Figure 3 can be given by[38]

$$E = IR_s + Q/C_s \quad (15)$$

or, after time-differentiation of (15), we get

$$\frac{dE}{dt} = I_o\omega R_s\cos(\omega t) + \frac{I_o}{C_s}\sin(\omega t) \quad (16)$$

Now, we have to equalize eqs 14 and 16 in order to identify R_s and C_s of the Faradaic element in Figure 3.

$$R_s = Z_{re} = R_{ct} + \frac{\beta_2}{zFA(1+K)\sqrt{2D\epsilon}} + \frac{1}{\sqrt{\omega}}\left[\frac{\beta_2}{zFA\sqrt{2D}}\frac{K}{(1+K)} + \frac{\beta_1}{zFA\sqrt{2D}}\right] \quad (17)$$

$$\frac{1}{\omega C_s} = -Z_{im} = \frac{1}{\sqrt{\omega}}\left[\frac{\beta_2}{zFA\sqrt{2D}}\frac{K}{(1+K)} + \frac{\beta_1}{zFA\sqrt{2D}}\right] + \frac{\beta_2}{zFA(1+K)\sqrt{2D\epsilon}} \quad (18)$$

where Z_{re} and Z_{im} are the real and imaginary parts of the impedance, respectively. If the kinetics of the ion transfer across the liquid−liquid interface is very fast, as often reported,[5,6] then the term R_{ct} would be very small in comparison with other terms, and eq 16 can be simplified to

$$R_s = Z_{re} = \frac{\beta_2}{zFA(1+K)\sqrt{2D\epsilon}} + \frac{1}{\sqrt{\omega}}\left[\frac{\beta_2}{zFA\sqrt{2D}}\frac{K}{(1+K)} + \frac{\beta_1}{zFA\sqrt{2D}}\right] \quad (19)$$

This means, for the considered facilitated ion transfer reactions, the variation of the real Z_{re} and imaginary part of the impedance Z_{im} with the inverse of the square-root of the frequency should be linear. The slope of those dependences (slopes should have same values, but opposite signs) can be used for estimation of the thermodynamic constant of the complexation constant K', since $K = 1/K'$. The intercepts hide also the values of the rate constants of the subsequent chemical reactions (i.e., k_f and k_b are hidden in ϵ).

Note that the values of Z_{im} and Z_{re} are experimentally obtained from the Nyquist plots.[20,38−42] In reality, the best linearity between Z_{re} and Z_{im} vs $\omega^{-1/2}$ is obtained in the region of low frequencies.[38] Equations 18 and 19 can always be used for the estimation of the complexation constant by the facilitated ion transfer reactions, provided that the value of the standard Gibbs energy of nonassisted ion transfer of the studied ion is known (this is needed in order to estimate the β_2 constant). These equations are very practical for the systems with kinetic hindrances by the interfacial complexation reaction, where cyclic voltammetry alone is incapable of providing the calculation of the thermodynamic parameters. Indeed, in such situations, the coupling of both CV and EIS is inevitable in order to fully understand the system behavior. Without knowing the voltammetric features of the system, the EIS is not self-sufficient to provide all demanded information of such systems.

3. Material and Methods

For the electrochemical measurements, the following chemicals were used as received: 1,2-dichloroethane (DCE; 99.9% Sigma), lithium chloride (LiCl; Aldrich 99%), tetraoctylammonium tetraphenylborate (TOATPB), sodium tetraphenylborate (NaTPB), and $Cu(NO_3)_2$. The compounds 2,8-dithia [9],(2,9)-1,10-phenanthrolinophane ($PhenS_2$) and 5-oxo-2,8-dithia [9],-(2,9)-1,10-phenanthrolinophane ($PhenOS_2$) were synthesized according to the procedure described in the literature.[43,44] Their structures are shown in Scheme 1. Mili Q-plus water (18 MΩ cm) was used for the preparation of all aqueous solutions, as well as for rinsing. All experiments were carried out at room temperature. The ITIES system consists of a four-electrode cell, with a flat water|DCE interface with an area of 0.28 cm^2:

Ag/AgCl | 50 mM NaTPB + 100 mM LiCl (w)| 50 mM TOATPB (DCE)+ x mM Ligand | 0.1 M LiCl + y mM Cu^{2+} (w) | AgCl/Ag

The voltammetric measurements at ITIES were carried out by applying the cyclic staircase voltammetry, with scan rates

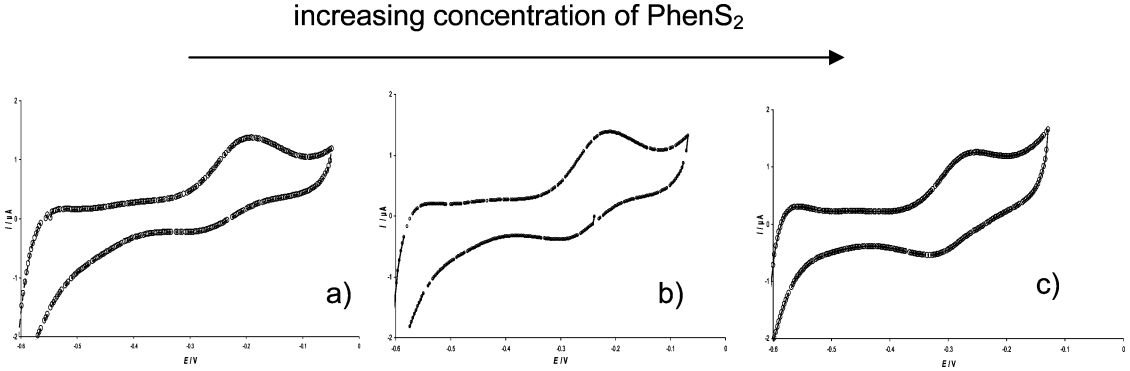

Figure 4. Effect of increasing the concentration of $PhenS_2$ in the organic phase on the mid-peak potentials of the cyclic voltammograms. $c(Cu^{2+})_w = 0.4$ mmol/L, and $c(PheS_2)_o$/mmol $L^{-1} = 0.2$ (a), 0.4 (b,) and 0.6 (c). "o" stands for organic phase and "w" for aqueous phase. Scan rate $\nu = 25$ mV/s.

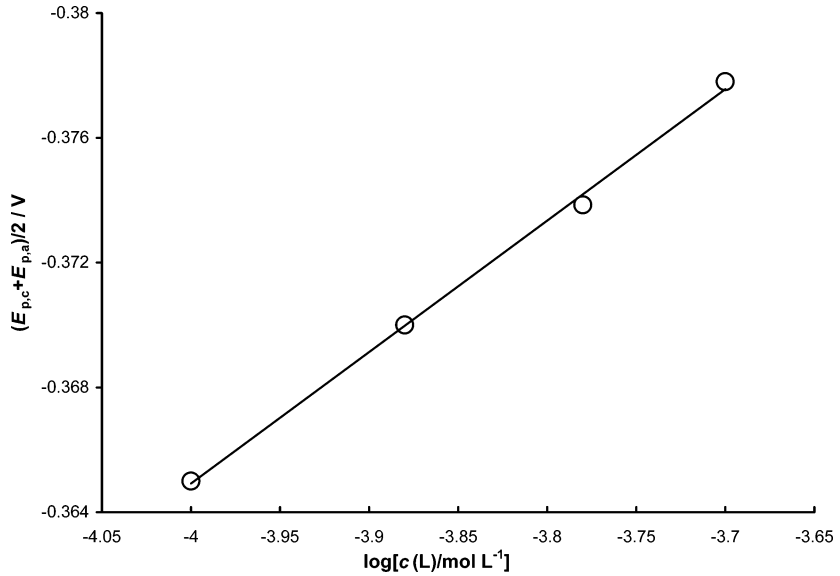

Figure 5. Dependence of peak mid-peak potential on the log(c(L)/mol L^{-1}). $c(Cu^{2+}) = 5$ mmol L^{-1}, (c(L) = 1 mmol L^{-1}). L is $PhenS_2$.

varying from 5 to 200 mV/s. All voltammograms have been measured using the Ohmic drop compensation mode.

4. Experimental Results

We present briefly here two experimental examples of FIT studied by cyclic voltammetry and of Cu^{2+} by interfacial complexation with two different phenanthroline-containing macrocyclic ligands ($PhenS_2$ and $PhenOS_2$) at the polarized water/1,2-dichloroethane interface, in order to relate the results obtained by theoretical simulations that are described above. It is well-known that various phenanthroline derivatives are often used as facilitating agents in assisted transfer of different metal ions across liquid−liquid interfaces.[15−17]

The reactions of $PhenS_2$ and $PhenOS_2$ with Cu^{2+} were also studied spectrophotometrically both in EtOH and in MeCN. Immediately upon mixing the reactants, a blue-green color is observed ($\lambda_{max} = 650$ nm). In time, this color disappears and solutions turn to yellow ($\lambda_{max} = 450$ nm). This behavior is observed for the two ligands, in both EtOH and in MeCN, and for solutions having different **L**/Cu^{2+} molar ratios (from 0.2 to 4). However, the blue-green color persists for several hours if the **L**/Cu^{2+} molar ratio is lower than 1.

Fast spectrophotometric titrations of Cu^{2+} with the ligands in EtOH or MeCN by recording the spectra immediately after mixing the reactants indicate a quantitative formation of $[Cu(\mathbf{L})]^{2+}$ complexes. Further addition of the ligands beyond the 1:1 **L**/Cu^{2+} molar ratio led to a gradual small decrease in absorbance at 650 nm, according to the observed instability of the species $[Cu(\mathbf{L})]^{2+}$ in the presence of excess ligands. However, the transformation of the blue-green species $[Cu(\mathbf{L})]^{2+}$ into those responsible for the yellow color is slow enough to allow both confirmation of their 1:1 stoichiometry by continuous variations plots, and calculation of their formation constants.

At the solid state, whatever the Cu^{2+}/**L** molar ratio used (1:1 or 1:2), the reaction between $PhenS_2$ and $PhenOS_2$ and $Cu(ClO_4)_2 \cdot 2H_2O$ in EtOH/CH_2Cl_2 always resulted in solid products containing the 1:1 complexes, as demonstrated by elemental analysis, FAB mass spectrometry, and X-structural analysis for $[Cu(PhenS_2O)(ClO_4)]ClO_4$. Several attempts were made to isolate 1:2 Cu^{2+}/**L** complexes at the solid state (presumably responsible for the yellow color in solution which develops on either adding excess ligands to the metal or allowing 1:1 metal-to-ligand mixture to stand) using different starting copper(II) metal salts and solvents. Only from the reaction of $PhenS_2$ with $CuCl_2 \cdot 2H_2O$, and after addition of excess of NH_4PF_6 to the reaction mixture, the complex $[Cu(PhenS_2)_2][PF_6]_2$ was separated as a red microcrystalline solid and unambiguously characterized by ESR to have a N_4 pseudotetrahedral coordination sphere around the metal center.[45] In the structurally characterized complex $[Cu(PhenS_2O)(ClO_4)]ClO_4$, the ligand adopts a folded conformation typical for these type of macrocycles with the aliphatic chain of the ring tilted over the plane

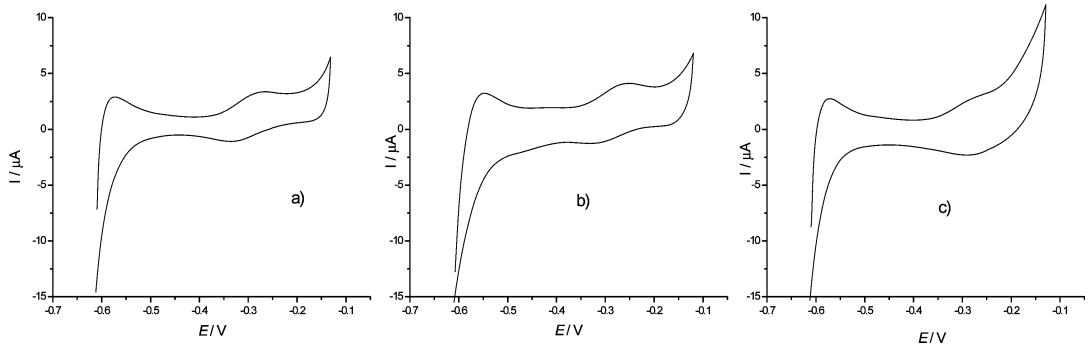

Figure 6. Effect of increasing the concentration of $PhenOS_2$ in the organic phase to the mid-peak potentials of the cyclic voltammograms. $c(Cu^{2+})_w = 0.3$ mmol/L, and $c(PheOS_2)_o$/mmol $L^{-1} = 0.2$ (a), 0.4 (b), and 0.6 (c). "o" stands for organic phase and "w" for aqueous phase. Scan rate $\upsilon =$ 25 mV/s.

containing the phenanthroline unit.[46] A pseudo-octahedral coordination sphere is reached at the metal center in by interaction of a perchlorate ion at the coordination site left free by the macrocycle.

Several cyclic voltammograms for the facilitated Cu^{2+} transfer, obtained when concentration of the ionophore 2,8-dithia [9],(2,9)-1,10-phenanthrolinophane ($PhenS_2$) in the organic solution is increased from 0.2 to 0.6 mmol/L, are shown in Figure 4. An increase of the ligand concentration in the organic phase leads to a shift of the mid-peak potential on the cyclic voltammograms toward negative direction, whereas the peak currents do not change upon the increase of the ligand concentration. The mid-peak potential is a linear function of $\log(c_{(L)})$, with a slope of -30 mV as shown in Figure 5. This slope is typical for the formation of a 1:1 complex, when the charge of the transferred ions is 2+.[18] The intercept of the linear relationship $(E_{p,c} + E_{p,a})/2$ vs $\log(c_{(L)})$ could serve as the estimation of the complexation constant K, providing that the value of the standard potential of non-assisted ion transfer of Cu^{2+} from water to 1,2-DCE is known.[8,18] When taking the value of $\Delta_w^{DCE}\varphi^{\theta}_{Cu^{2+}} = -0.56$ V,[47] the estimated value of complexation constant of Cu^{2+} and $PhenS_2$ is $\log(K) = 13.25$ (tetramethylammonium has been used as an internal standard for these experiments). Obviously, these experimental results comply well with the theoretical voltammograms simulated for the case of the absence of kinetic effects (see Figure 1), and the Nernstian approaches[5,18,21,23] can be applied for the estimation of the thermodynamic parameters.

The cyclic voltammograms for the assisted Cu^{2+} transfer recorded in presence of 5-oxo-2,8-dithia [9],(2,9)-1,10-phenanthrolinophane ($PhenOS_2$; see Figure 6) show, however, opposite behavior compared to the previous example. In this case, the mid-peak potentials of the cyclic voltammograms are insensitive to the increase of the ligand concentration in the organic phase. Moreover, the shapes of the voltammograms have features typical for systems where chemical kinetic effects are present (compare with voltammograms in Figure 2). In this case, the cyclic voltammetry is not effective tool for thermodynamic estimations, and more detailed analysis under EIS conditions is required,[20] in order to full characterization of the system under investigation. Shown in the Figure 7 are the dependences of the real and imaginary part of the impedance on the inverse of the square-root frequency (in the low-frequency region), for the system of Cu^{2+} transfer facilitated by $PhenOS_2$ ligand, measured at equilibrium potential. Obviously, a linear relationship between both parameters exists, as predicted by the evaluated eqs 17 and 18. Moreover, both slopes are almost identical, but with opposite signs, as predicted by eqs 17 and 18. By substituting the slopes of the dependences from Figure 7 into the corresponding eqs 17 and 18, we estimated that the value of the thermodynamic constant of the complexation reaction between Cu^{2+} and $PhenOS_2$ is $\log(K) = 17.02$ (T of 298 K, and $D = 5 \times 10^{-6}$ cm^2 s^{-1}). It is important to stress that for these estimations, we used the value for the non-assisted ion transfer of Cu^{2+} $\Delta_w^{DCE}G^{\theta}_{Cu^{2+}} = 110$ kJ/mol, provided from the work of Girault et al. .[47] Therefore, these estimations significantly depend on the accuracy of the determined values of the standard Gibbs energies of non-assisted ion transfers.

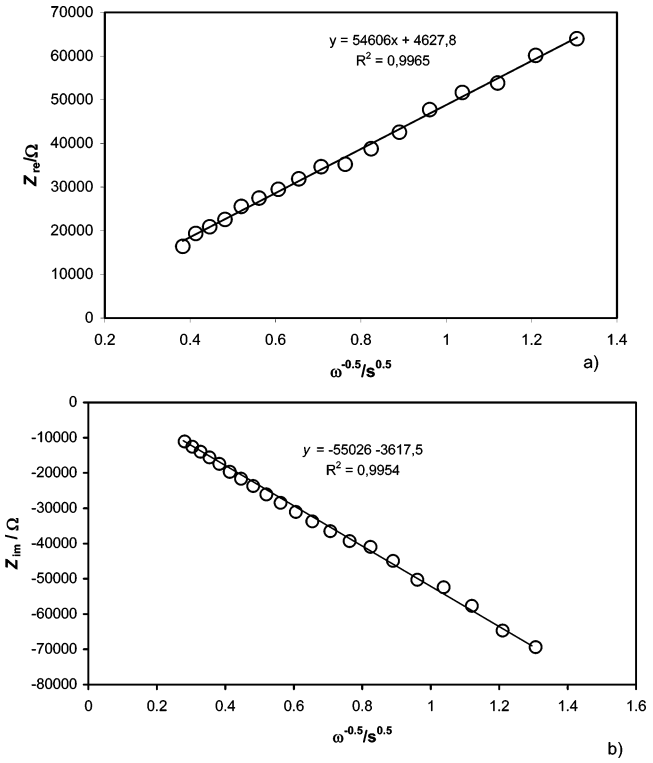

Figure 7. Dependence of the real (a) and imaginary part (b) of the impedances vs the inverse of the square-root frequency for the facilitated transfer of Cu^{2+} with ligand $PhenOS_2$ (in the low-frequency region). The Nyquist plots have been recorded at equilibrium potential, with frequency varying from 0.5 to 200 s^{-1}. $c(Cu^{2+})_w = 0.5$ mmol/L, $c(PhenOS_2)_o = 0.6$ mmol L^{-1}, $T = 298$ K.

6. Conclusions

Although the kinetic effects due to the presence of hindrances by the chemical step in the case of facilitated ion transfer processes are often encountered in many experimental situations, only a minor attention has been paid to them so far. We give here simple theoretical qualitative criteria under conditions of

cyclic voltammetry for recognition of these effects. Moreover, we present a corresponding mathematical model solved under conditions of electrochemical impedance spectroscopy, while providing analytical equations that can be used for elucidation of the thermodynamics and kinetics of the follow-up chemical reactions in such systems. Although these effects qualitatively resemble those observed in the case of slow kinetic due to the ion transfer step, they fundamentally differ with respect to some parameters that determine them. The monitoring of the features of cyclic voltammograms by variation of the ligand concentration can serve as a simple criterion for recognizing the kinetic effects due to the complexation reaction in the FIT processes. Neglecting these effects will give wrong values for the estimated thermodynamic parameters. It is worth noting that the scan rate in cyclic voltammetric experiments affects simultaneously both kinetics, i.e., that of the ion transfer, and that due to the complexation reaction.[20,22,35] Therefore, the scan rate dependence can often lead to misinterpretations, if both kinetic effects are present by the facilitated ion transfer processes. Note once again, that the estimated values of the thermodynamic parameters from the proposed EIS model, by using eqs (17−19) of this work, depend significantly on the values of the standard Gibbs energies of non-assisted ion transfers. While these values for the monocharged ions are easily accessible from various voltammetric experiments,[3−6] there are lots of uncertain values reported for the double-charged ions, and those should be always taken with cautions. Nevertheless, for experimental systems as those elaborated in this work, neither EIS nor cyclic voltammetry are self-sufficient techniques, and they must be coupled for complete clarification of the problems.

Acknowledgment. R.G. acknowledges the FCT of Portugal for the postdoctoral fellowship Grant SFRH/BPD/14894/2004.

References and Notes

(1) Senda, M.; Kakiuchi, T.; Osakai, T. *Electrochim. Acta* **1991**, *36*, 253.

(2) Samec, Z. *Pure Appl. Chem.* **2004**, *76*, 2147.

(3) Testa, B.; van de Waterbeemd, H.; Folkers, G.; Gay, R. *Pharmacokinetic Optimization in Drug Research*; Wiley-WCH: Weinheim, Germany, 2001.

(4) Scholz, F.; Schroeder, U.; Gulaboski, R. *Electrochemistry of Immobilized Particles and Droplets*; Springer: Berlin, 2005.

(5) Volkov, A. G. *Liquid Interfaces in Chemical, Biological and Pharmaceutical Applications*; Marcel Dekker: New York, 2001.

(6) Girault, H. H.; Schiffrin, D. J. *Electroanal. Chem.*: *A Series of Advances*; Bard,A. J., Ed.; Marcel Dekker: New York, 2000; Vol 15, pp 1−132.

(7) Bakshi, M. S.; Doe, H.; Sakurada, N.; Arakawa, R. *Chem. Lett.* **1999**, *10*, 1059.

(8) Tomaszewski, L.; Lagger, G.; Girault, H. H. *Anal. Chem.* **1999**, *71*, 837.

(9) Han, X.; Zhang, Z.; Dong, S.; Wang, E. *Electroanalysis* **2004**, *16*, 1014.

(10) Shao, Y.; Osborne, M.; Girault, H. H. *J. Electroanal. Chem.* **1991**, *308*, 101.

(11) Kong, Y.-T.; Imabayashi, S.; Kakiuchi, T. *J. Am. Chem. Soc.* **2000**, *122*, 8215.

(12) Kong, Y.-T.; Kakiuchi, T. *J. Electroanal. Chem.* **1998**, *446*, 19.

(13) Baruzzi, A. M.; Wendt, H. *J. Electroanal. Chem.* **1990**, *279*, 19.

(14) Fernandez, M. A.; Yudi, L. M.; Baruzzi, A. M. *J. Electroanal. Chem.* **2001**, *505*, 165.

(15) Doe, H.; Hoshiyama, M.; Jian, L. *Electrochim. Acta* **1995**, *40*, 2947.

(16) Dassie, S. A.; Yudi, L. M.; Baruzzi, A. M. *Electrochim. Acta* **1995**, *40*, 2953.

(17) Ferreira, E. S.; Garau, A.; Lippolis, V.; Pereira, C. M.; Silva, F. *J. Electroanal. Chem.* **2006**, *587*, 155.

(18) Reymond, F.; Lagger, G.; Carrupt, P.-A.; Girault, H. H. *J. Electroanal. Chem.* **1998**, *451*, 59.

(19) Reymond, F.; Fermin, D.; Lee, H.; Girault, H. *Electrochim. Acta* **2000**, *45*, 2647.

(20) Gulaboski, R.; Pereira, C. M.; Cordeiro, M. N. D. S.; Bogeski, I.; Ferreira, E.; Ribeiro, D.; Chirea, M.; Silva, A. F. *J. Phys. Chem. B* **2005**, *109*, 12549.

(21) Beattie, P. D.; Wellington, R. G.; Girault, H. H. *J. Electroanal. Chem.* **1995**, *396*, 317.

(22) Garay, F.; Lovric, M. *J. Electroanal. Chem.* **2002**, *518*, 91.

(23) Homolka, D.; Holub, K.; Marecek, V. *J. Electroanal. Chem.* **1982**, *138*, 29.

(24) Wandlowsky, T.; Marecek, V.; Samec, Z. *J. Electroanal. Chem.* **1988**, *242*, 291.

(25) Manzanares, M. V.; Schiffrin, D. J. *Electrochim. Acta* **2004**, *49*, 4651.

(26) Beattie, P. D.; Delay, A.; Girault, H. H. *Electrochim. Acta* **1995**, *40*, 2961.

(27) Sun, P.; Zhang, Z.; Gao, Z.; Shao, Y. *Angew. Chem. Int. Ed.* **2002**, *41*, 3445.

(28) Fernandez, M. A.; Yudi, M.; Baruzzi, A. M. *Electroanalysis* **2004**, *16*, 491.

(29) Shao, Y. S.; Tan, N.; Devaud, V.; Girault, H. H. *J. Chem. Soc. Faraday Trans.* **1993**, *89*, 4307.

(30) Cheng, Y.; Schiffrin, D. J. *J. Electroanal. Chem.* **1997**, *429*, 37.

(31) Dassie, S. A.; Yudi, L. M.; Baruzzi, A. M. *Electrochim. Acta* **1995**, *40*, 2953.

(32) Katano, H.; Osakai, T.; Himeno, S.; Saito, A. *Electrochim. Acta* **1995**, *40*, 2935.

(33) Ding, J.; Hotta, H.; Osakai, T. *J. Electroanal. Chem.* **2001**, *505*, 133.

(34) Nicholson, R. S.; Shain, I. *Anal. Chem.* **1964**, *36*, 706.

(35) O'Dea, J. J.; Osteryoung, J.; Osteryoung, R. A. *Anal. Chem.* **1981**, *53*, 695.

(36) Nicholson, R. S.; Olmstead, M. L. In *Electrochemistry: calculations, simulation and instrumentation*; Mattson, J. S., Mark, H. B., MacDonald, H. C., Eds.; Dekker: New York, 1972; Vol. 2, pp 120−137.

(37) Mirceski, V.; Gulaboski, R.; Kuzmanovski, I. *Bull. Chem. Technol. Macedonia* **1999**, *18*, 57. (pdf available online at: www.tmf.ukim.edu.mk/bulletin/trud.php?id=38&jd=21&start=5).

(38) (a) Barsoukov, E.; MacDonald, J. R. *Impedance Spectroscopy, Theory, Experiments and Applications*; Wiley: New York, 2005. (b) Bard, A. J.; Faulkner, L. R. Techniques based on concepts of Impedance. In *Electrochemical Methods, Fundamentals and Applications*; Wiley & Sons: New York, 2001; p 368.

(39) Sluyters-Rehbach, M.; Sluyters, J. H. *J. Electroanal. Chem.* **1969**, *23*, 457.

(40) Sluyters-Rehbach, M.; Sluyters, J. H. *J. Electroanal. Chem.* **1970**, *26*, 237.

(41) Prieto, F.; Rueda, M.; Navarro, I.; Sluyters-Rehbach, M.; Sluyters, J. H. *J. Electroanal. Chem.* **1996**, *405*, 1.

(42) Smith, D. E. *Anal. Chem.* **1963**, *35*, 602.

(43) Arca, M.; Blake, A. J.; Casabó, J.; Demartin, F.; Devillanova, F. A.; Garau, A.; Isaia, F.; Lippolis, V.; Kivekas, R.; Muns, V.; Schröder, M.; Verani, G. *J. Chem. Soc., Dalton Trans.* **2001**, 1180.

(44) Aragoni, M. C.; Arca, M.; Demartin, F.; Devillanova, F. A.; Isaia, F.; Garau, A.; Lippolis, V.; Jalai, F.; Papke, U.; Shamsipur, M.; Tei, L.; Yari, A.; Verani, G. *Inorg. Chem.* **2002**, *41*, 6623.

(45) Arca, M.; Azimi, G.; Demartin, F.; Devillanova, F. A.; Escriche, L.; Garau, A.; Isaia, F.; Kivekas, R.; Lippolis, V.; Muns, V.; Perra, A.; Shamsipur, M.; Sportelli, L.; Yari, A. *Inorg. Chim. Acta* **2005**, *358*, 2403.

(46) Lippolis, V.; Shamsipur, M. *J. Iran. Chem. Soc.* **2006**, *3*, 105.

(47) Lagger, G.; Tomaszewski, L.; Osborne, M. D.; Seddon, B. J.; Girault, H. H. *J. Electroanal. Chem.* **1998**, *451*, 29.